Supplementary Methods

Real-time RT- PCR. Total RNA was isolated from kidneys of 8-week-old WT and IEX-1 KO mice and reverse-transcribed to cDNA. Erythropoietin mRNA was quantified by real-time RT-PCR and normalized against 18S rRNA as described[11]. The primers were 5′-CAT CTG CGA CAG TCG AGT TCTG-3′ (forward) and 5′-TGC ACA ACC CAT CGT GAC AT-3′ (reverse) for mouse erythropoietin; and 5′-TCG AGG CCC TGT AAT TGG AA-3′ (forward) and 5′-CCC TCC AAT GGA TCC TCG TT-3′ (reverse) for mouse 18S. For human blood samples, total RNA was isolated from whole blood cells using the QIAamp RNA blood mini kit (Qiagen). RNA was reverse-transcribed with a high capacity RNA-to-cDNA kit (Applied Biosystems). Real-time PCR was performed on Roche Lightcycler 480 with a SYBR Green I Master kit (Roche Diagnostics). Relative quantity of IEX-1 expression was normalized to human 18S rRNA, and calculated using comparative Ct method (ΔΔCt method). The primers were 5′-CGC AGC CGC AGG GTT CTC TA-3’ (forward) and 5′-CGG GTG TTG CTG GAG GAA AG-3′ (reverse) for IEX-1; and 5′- TCA ACT TTC GAT GGT AGT CGC CGT-3′ (forward) and 5′-TCC TTG GAT GTG GTA GCC GTT TCT -3′ (reverse) for 18S rRNA.

Flow cytometry. Reticulocytes and erythroblasts were stained with FITC-anti-CD71 and PE-anti-Ter119 (BioLegend). Some cells were also incubated with 200 nM MitoTracker (Molecular Probes) to stain mitochondria. To analyze $\Delta\psi_m$, cells were incubated with 10 μg/ml tetraethylbenzimidazolylcarbocyanine iodide (JC1, Molecular Probes) following PerCP/Cy5.5-anti-Ter119 and PE/Cy7-anti-CD71 (BioLegend) staining, and the red J-aggregate fluorescence at 590 nm was analyzed by flow cytometry. Intracellular ROS were measured with 10 μM CM-H2DCFDA (Molecular Probes) following PerCP/Cy5.5-anti-Ter119 and PE/Cy7-anti-CD71 staining.

Transmission electron microscopy. Cells were pelleted and fixed in Karnovsky’s fixative at 4°C for overnight. The pellets were washed with 0.1 M sodium cacodylate buffer, postfixed in 2% OsO_4 in sodium cacodylate buffer, dehydrated, and embedded in Epon t812 (Tousimis). Ultrathin sections were cut, stained, and examined on a Philips CM-10 transmission electron microscope (Eindhoven). Images were recorded with an undermount XR41M 4 Mpixel cooled camera.

Immunofluorescence staining for autophagosomes. Sorted young reticulocytes were cultured on a Poly-D-Lysine coated coverslip in culture medium. At indicated time, cells were fixed with 4% paraformaldehyde and permeabilized with 0.1% (wt/vol) saponin (Sigma) for 15 min. The cells were incubated for overnight at 4°C with mouse anti-COX IV and a rabbit antibody against LC3 (BD Bioscience), followed with Alexa Fluor-conjugated secondary antibody (BD Bioscience) for 30 min at 37°C. The cells were examined using Olympus FV1000 confocal microscope. Acquired images from 6-9 different samples in each group were then analyzed using FV10-ASW 4.0 Viewer software (Olympus).

Isolation and quantification of reticulocyte-secreted exosomes. $Ter119^{+}CD71^{high}$ reticulocytes were sorted from WT and KO mice as above and cultured at a density of $1x10^{7}$ cells in 10 ml culture medium for 2 days. The culture media were collected on ice and centrifuged at 800 x *g* for 10 min to pellet the cells, and then at 12,000 x *g* for 30 min to remove cellular debris. Exosomes were collected from the supernatant by centrifugation at 100,000 x *g* for 2 hr. The exosome pellet was washed once and resuspended in 100 μl PBS. The mount of released exosomes was quantified by the activity of acetylcholinesterase using a QuantiChrom Acetylcholinesterase Assay Kit (BioAssay Systems). Briefly, 10 μl of exosome fraction were incubated with 190 μl Working Reagent in a clear bottom 96-well plate at 37°C. The absorbance at 412 nm was recorded at 2 and 10 min after incubation. The acetylcholinesterase activity was calculated according to the manufacturer's protocol, and one unit was defined as the enzyme catalyzed the production of 1 μmole of thiocholine per minute under the assay conditions. In a separate experiment, exosomes were lysed by NP-40 buffer and subjected to iron determination.

Various routine methods. Peripheral blood smears were stained with Wright-Giemsa (Sigma) or new Methylene blue (Poly Scientific) according to the manufacturer's protocol. Microscopic analysis was conducted with a Zeiss Axiophot and images were captured using Picture Frame 2.3 software. For complete blood cell count, 50 μl of mouse blood was collected via retro-orbital puncture into an EDTA-coated microtainer tube (BD Bioscience) and analyzed on a HemaTrue veterinary hematology analyzer (Heska Corporation). The number of experiments (including biological and technical replicates) is defined in each figure legend.

Mice. All mice were used at 8~12 weeks of age and gender-matched. All mice were randomly divided to different experiment groups, and the numbers of mice are outlined in each figure legend. The sample size was determined using power analysis to give a statistical power of >90% and standard deviation of 0.1 based on the expected experiment result at alpha = 0.05. Investigators were blinded to the all cell and mouse treatment groups. All outliers of study subjects were included in the data analysis.

Primary human samples. Reticulocytes of human peripheral blood samples were stained with FITC-anti-CD235a and PE-anti-CD71. Mitochondria in human RBCs were stained with 200 nM MitoTracker Deep Red FM before the cells were identified with FITC-anti-CD235a and PE-anti-CD71 (BD Bioscience). Mitochondrial membrane potential $\Delta\psi_m$ in human RBCs were labeled with 10 μg/ml JC1 and then with PerCP/Cy5.5-anti-CD235a and PE/Cy7-anti-CD71 (BioLegend). Similarly, human RBCs were identified with PerCP/Cy5.5-anti-CD235a and PE/Cy7-anti-CD71 and then incubated with 10 μM CM-H2DCFDA to measure intracellular ROS.

Supplementary Figure

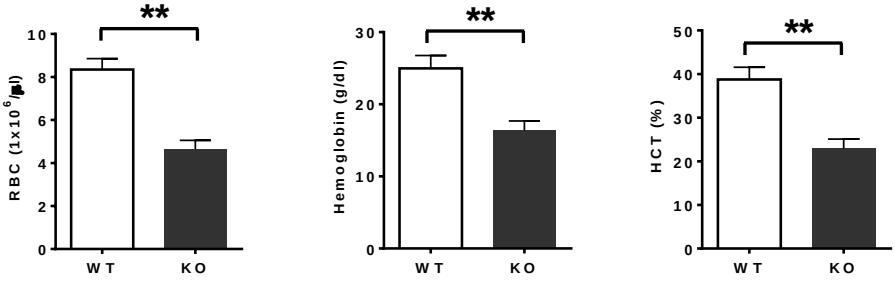

Figure S1. Deficient erythropoiesis of IEX-1 KO mice. Complete blood cell (CBC) counts were determined at 3 days after PHZ (100mg/kg) injection. KO mice exhibited lower levels of RBCs (49%), hemoglobin (34%), and hematocrit (41%) than WT mice. Data represent mean ± SEM (n = 12): **P<0.01 compared between WT and KO mice.

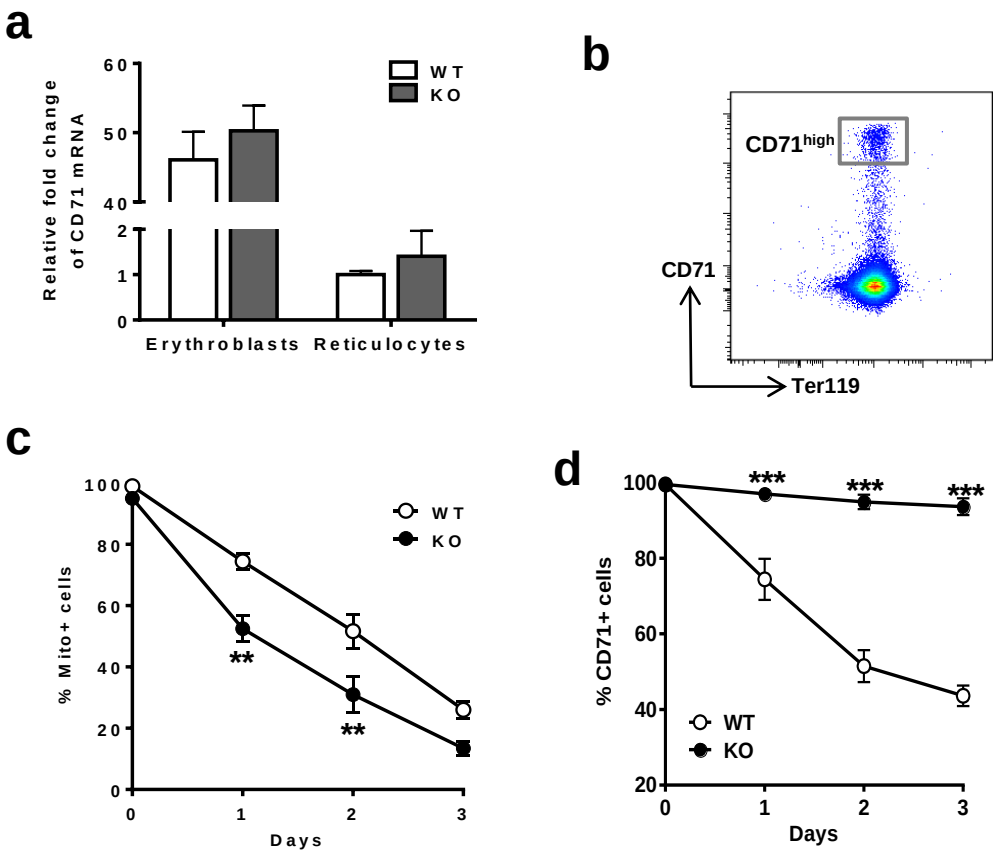

Figure S2 Uncoupling of mitochondrial clearance with CD71 shedding in IEX-1 KO reticulocytes during maturation. (**a**) Unaltered CD71 transcription in the absence of IEX-1. Quantitative RT-PCR of CD71 in indicated cells showed no difference in the presence or the absence of IEX-1 (n=9). **(b)** $Ter119^{+}CD71^{high}$ reticulocytes were sorted from WT and KO mice at day 3 after PHZ treatment for *ex vivo* maturation. (**c,d**) Accelerated mitochondrial clearance (**c**) and delayed CD71 shedding (**d**) in IEX-1 KO reticulocytes during their maturation. MFI of MitoTraker (**c**) and PE-conjugated CD71 (**d**) were plotted vs. time and expressed as mean ± SEM (n=12), **P<0.01 and ***P<0.001 compared with WT groups.

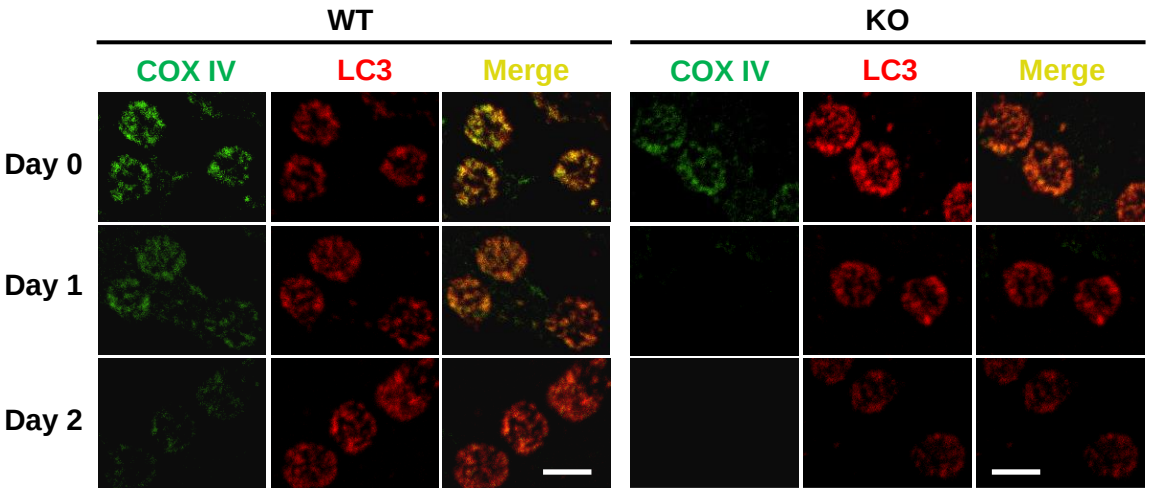

Figure S3. Enhanced autophagy in KO young reticulocytes. Autophagosomes were marked by microtubule-associated protein light chain 3 (LC3). KO reticulocytes had more LC3 punctates at the initiation of culture (LC3 punctates per cell: WT, 16.1± 2.7; KO, 21.8±2.5; $P<0.01$), but fewer mitochondria marked by mitochondrial complex IV (COXIV) staining. Representative results of at least 12 samples per group are shown.

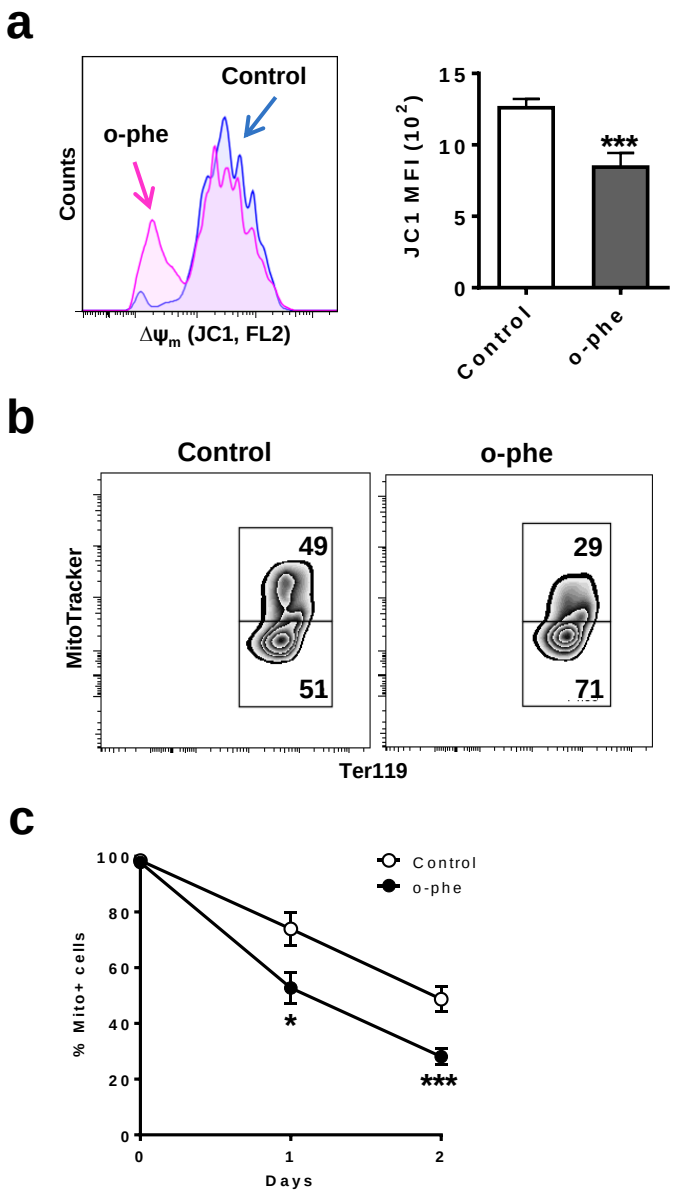

Figure S4. O-phenanthroline increases mitochondrial clearance in WT reticulocytes. WT Ter119^{+}CD71^{high} reticulocytes were sorted and cultured as Fig. 2d in the presence of 1 μM o-phenanthroline. The inhibitor reduced mitochondrial membrane potential as measured by JC1 staining at 24 hr post-incubation (**a**). The mitochondrial mass was determined on day 2 after incubation (**b**), and plotted against time , *P<0.05 and ***P<0.001 compared with untreated controls.

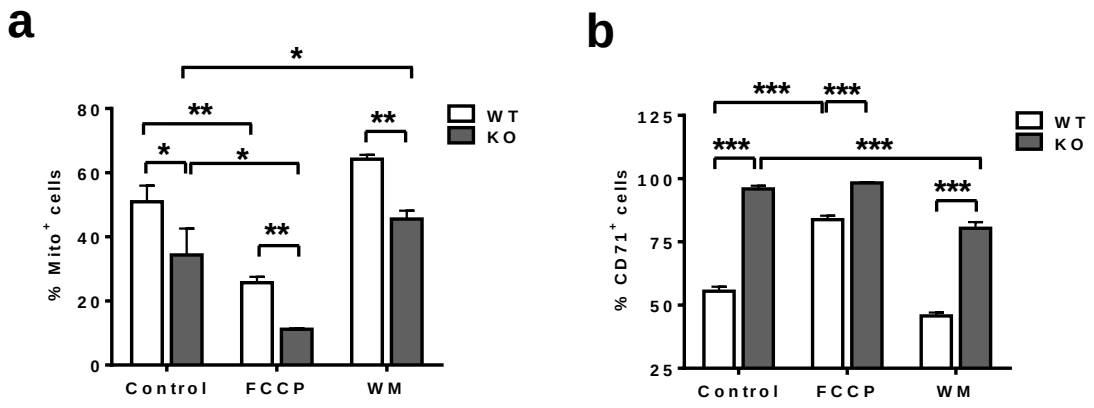

Figure S5. Modulation of mitochondrial autophagy affects CD71 shedding during reticulocyte maturation. Ter119^{+}CD71^{high} reticulocytes were sorted and cultured in the presentence of 10 μM FCCP or 100 nM WM as Figure **3c**. The cells were stained with MitoTracker and PE-conjugated CD71 at 2 days after *ex vivo* maturation. The percentages of cells containing mitochondria (**a**) and CD71 (**b**) were shown as mean ± SEM (n=12), *P<0.05, **P<0.01 and ***P<0.001 compared between indicated groups.

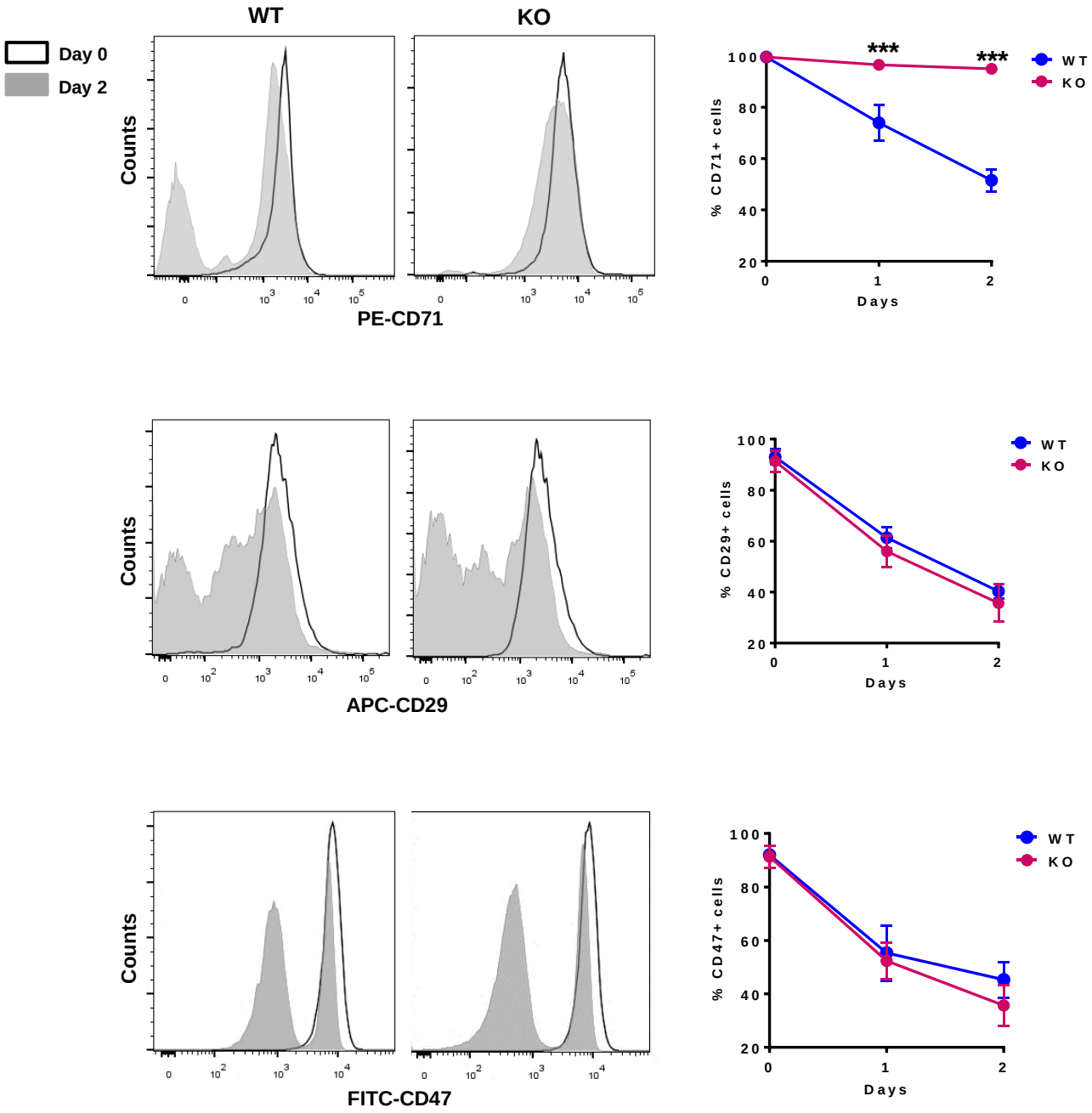

Figure S6. Reduced shedding of CD71 but not other proteins in IEX-1 KO reticulocytes. Young reticulocytes were sorted and subjected to 2-day ex vivo maturation as Fig. 2d. CD71, CD29 and CD47 on the cell surface were analyzed daily by flow cytometry after staining with corresponding antibodies. The right panels are histograms of flow cytometric analysis of each protein. Black lines, day 0 and grey, day 2. The left panels are sum of the flow cytometric data (n=5). There was no difference in the clearance of CD29 or CD47 between WT and KO reticulocytes. ***P<0.001 compared between WT and KO groups.

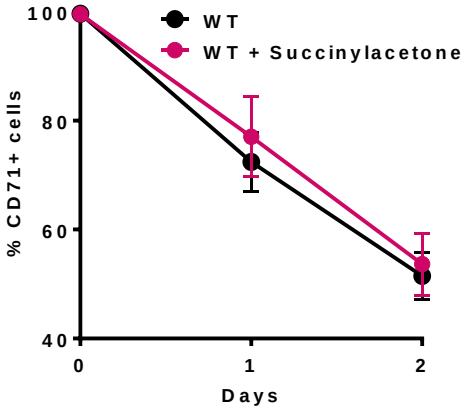

Figure S7. Inhibition of heme synthesis by succinylacetone doesn't impair CD71 shedding in WT reticulocytes. Ter119^{+}CD71^{high} reticulocytes were sorted from WT mice and cultured in the presence of 1mM succinylacetone. The percentage of CD71^{+} cells was determined on indicated days as mean ± SEM (n=5).

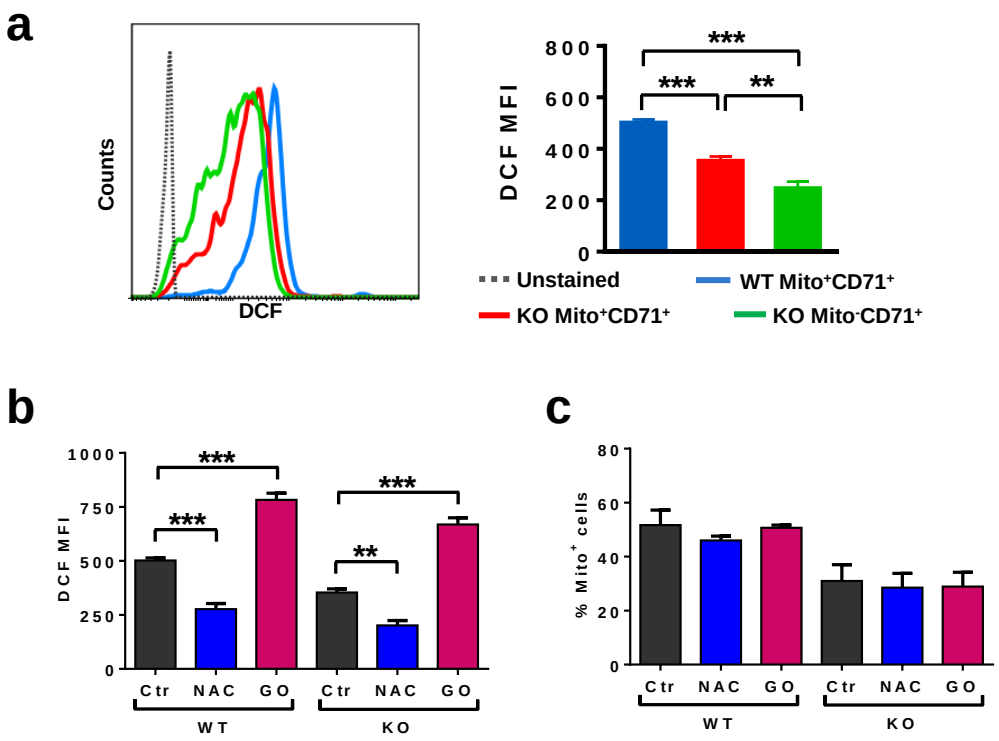

Figure S8. Effects of ROS production on reticulocyte maturation. (**a**) ROS levels are significantly decreased in KO reticulocytes in comparison with WT counterparts, especially in KO reticulocytes devoid of mitochondria. (**b,c**) $Ter119^{+}CD71^{high}$ reticulocytes as Figure 4f were cultured in the presence of 5 μM NAC or 5 mU/mL GO and stained with DCF to measure ROS at 6 hr after initial culture (**b)** or with Mitotraker at the end of 2-day *ex vivo* maturation (**c**). Data are expressed as mean ± SEM (n=9). **P<0.01 and ***P<0.001 compared between indicated groups.

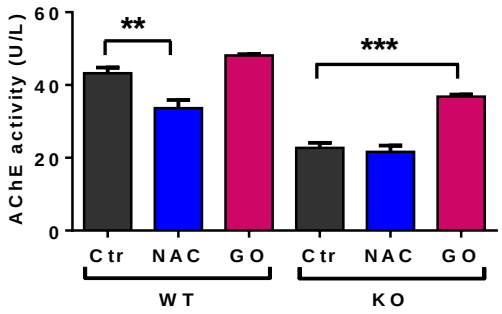

Figure S9. Quantification of exocytosis activity after NAC/GO treatment. Young reticulocytes were sorted and cultured as Fig. 4j. On day 2, secreted exosomes from $1x10^7$ reticulocytes were determined by the activity of AChE. Data are expressed as mean ± SEM (n=12). **P<0.01 and ***P<0.001 compared between indicated groups.

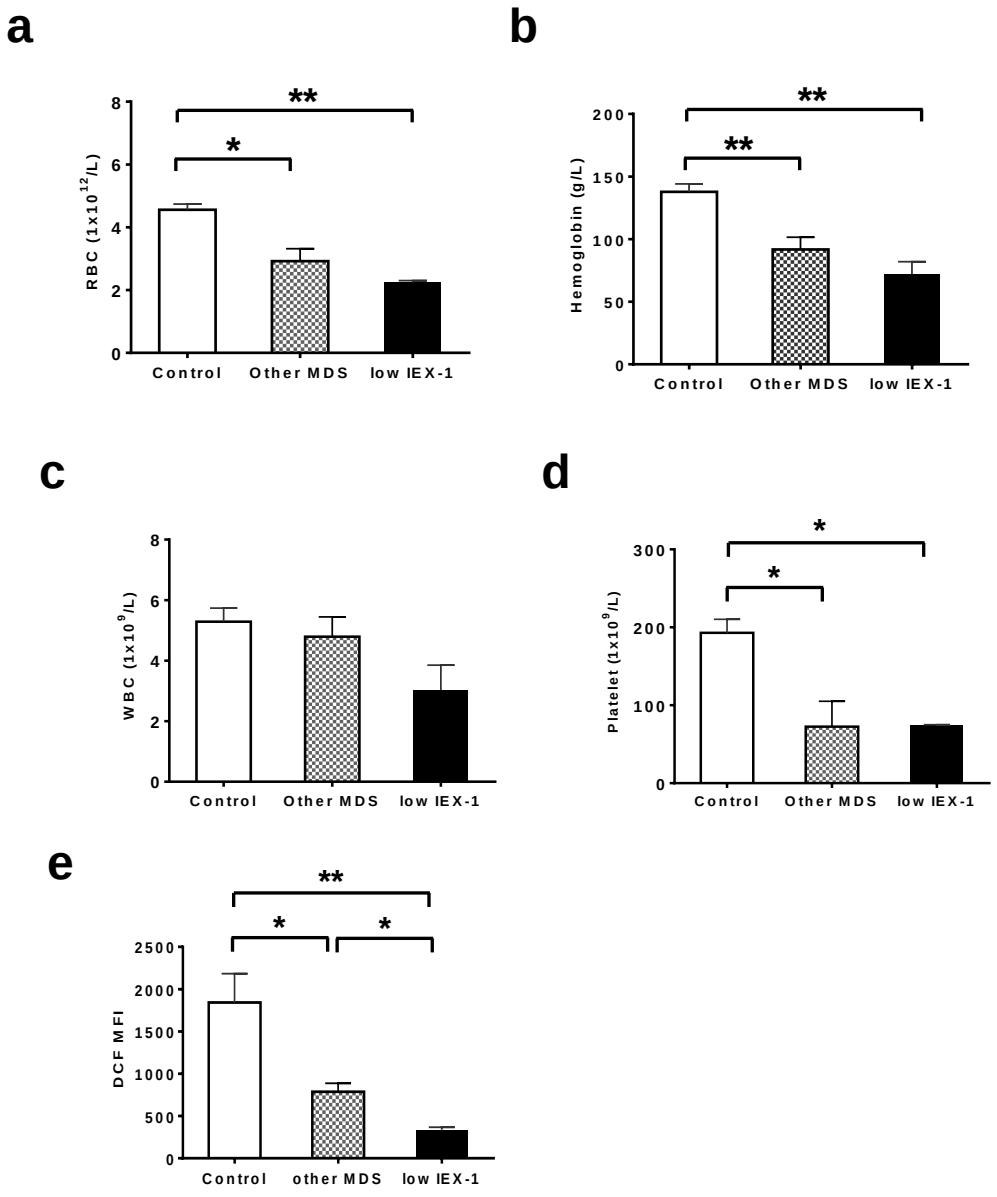

Figure S10. CBC counts and ROS level in MDS patients. (**a-d**) Complete blood cell counts of part of the samples in Fig. 5 are shown. (**e**) Reduced ROS in reticulocytes of MDS patients. Cellular ROS level of CD235a+ CD71+ reticulocytes were analyzed by flow cytometry using DCF staining. Healthy control n=5; other MDS n=8; MDS with low IEX-1 n=3. Data represent mean ± SEM, *P<0.05 and **P<0.01 compared between indicated groups.

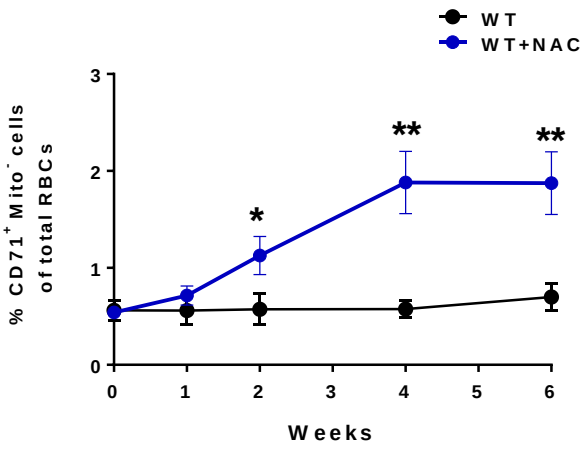

Figure S11. CD71^{+}Mito^{-} reticulocytes increase in WT mice after NAC injection. NAC (100 mg/kg) was i.p. injected 3 times per week for 6 weeks. The proportion of CD71^{+}Mito^{-} cells relative to total Ter119^{+} RBCs increased progressively over time: week 0, 0.54%; week 2, 1.13%; week 4, 1.88%; and week 6, 1.88%. Data represent mean ± SEM, *P<0.05 and **P<0.01 compared to sham-treated controls. n=12 in each group.

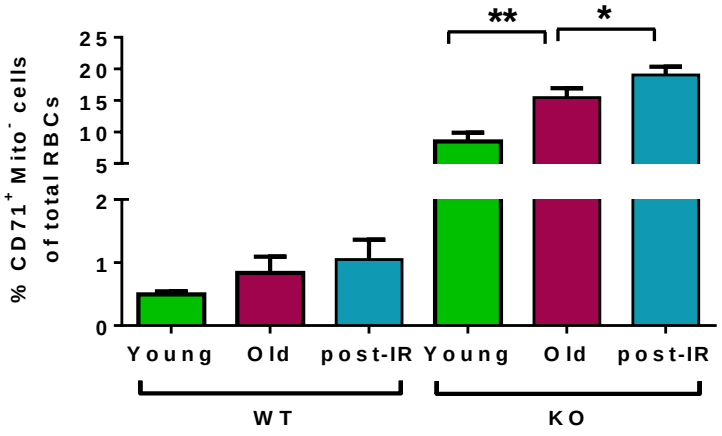

Figure S12. CD71^{+}Mito^{-} reticulocytes increase as animals age or after irradiation. The proportions of CD71^{+}Mito^{-} cells in total Ter119^{+} RBCs were measured in blood. Although there was a trend of increasing CD71^{+}Mito^{-} cells, no statistical difference was found in WT mice. In KO mice, the percentage increased from 8.5% in young mice to 15.4% in old mice, and to 19.0% in irradiated (IR) adult mice. Young mice, 4-week old; Old mice, 8-month old; and post-IR mice, 3Gy IR given to 3-month-old mice and then check the blood 5 months after IR. Data represent mean ± SEM, *P<0.05 and **P<0.01 between indicated groups. n=9 in each group.